© 2019. Published by The Company of Biologists Ltd | Journal of Experimental Biology (2019) 222, jeb200899. doi:10.1242/jeb.200899

RESEARCH ARTICLE

Vision is highly sensitive to oxygen availability in marine invertebrate larvae

Lillian R. McCormick[1,*], Lisa A. Levin[1] and Nicholas W. Oesch[2,3]

ABSTRACT

For many animals, evolution has selected for complex visual systems despite the high energetic demands associated with maintaining eyes and their processing structures. Therefore, the metabolic demands of visual systems make them highly sensitive to fluctuations in available oxygen. In the marine environment, oxygen changes over daily, seasonal and inter-annual time scales, and there are large gradients of oxygen with depth. Vision is linked to survival in many marine animals, particularly among the crustaceans, cephalopods and fish, and early life stages of these groups rely on vision for prey capture, predator detection and their distribution in the water column. Using *in vivo* electroretinogram recordings, we show that there is a decrease in retinal sensitivity to light in marine invertebrates when exposed to reduced oxygen availability. We found a 60–100% reduction in retinal responses in the larvae of cephalopods and crustaceans: the market squid (*Doryteuthis opalescens*), the two-spot octopus (*Octopus bimaculatus*), the tuna crab (*Pleuroncodes planipes*) and the graceful rock crab (*Metacarcinus gracilis*). A decline in oxygen also decreases the temporal resolution of vision in *D. opalescens*. These results are the first demonstration that vision in marine invertebrates is highly sensitive to oxygen availability and that the thresholds for visual impairment from reduced oxygen are species-specific. Oxygen-impaired retinal function may change the visual behaviors crucial to survival in these marine larvae. These findings may impact our understanding of species' vulnerability to ocean oxygen loss and suggest that researchers conducting electrophysiology experiments should monitor oxygen levels, as even small changes in oxygen may affect the results.

KEY WORDS: Zooplankton, Phototransduction, Physiology, Electroretinogram, Hypoxia

INTRODUCTION

Phototransduction is the process by which the energy from photons of light is translated into neural signals by photoreceptor cells (Rayer et al., 1990). The neural signaling requires the constant depolarization and repolarization of photoreceptors and downstream neurons, making vision one of the most energetically expensive processes in many animal systems (Ames, 2000; Pepe, 2001). These metabolic demands increase as temporal and spatial resolution increase and the visual system becomes more complex (Niven and Laughlin, 2008; Wong-Riley, 2010). As in terrestrial vertebrates, many marine invertebrates possess complex visual systems with a range of contrast and light sensitivities as well as sufficient temporal resolution for executing vital tasks such as prey capture or predator evasion (Warrant and Johnsen, 2013). One technique used to measure visual physiology is the electroretinogram (ERG), which records the summed activity of photoreceptors and downstream neurons in the eye in response to visual stimulation (Brown, 1968). The ERG is commonly used to measure the response of retinas in both vertebrate (Brown, 1968; Chen and Stark, 1994; Chrispell et al., 2015) and invertebrate systems (Cohen et al., 2015; Cronin and Forward, 1988; Frank, 1999; Lange and Hartline, 1974). Oxygen effects on vision have been extensively studied in humans and other terrestrial vertebrates, where a decline in oxygen (hypoxia) is known to cause a decrease in both sensitivity to light (Linsenmeier et al., 1983; McFarland and Evans, 1939) and temporal resolution (Fowler et al., 1993). In these vertebrate experiments, diminished sensitivity to light is demonstrated by a decrease in amplitude of visual responses after exposure to lower levels of oxygen, whereas reduced temporal resolution is seen as an inability of the retina to respond to high-frequency flashes of light. Both light and sufficient levels of oxygen are thus required for normal visual function.

In the marine environment, large gradients of irradiance and oxygen exist with depth, and changes in the partial pressure of oxygen (P_{O_2}) with water depth in the ocean can be up to 10-fold greater than the changes in atmospheric P_{O_2} over terrestrial altitude (McCormick and Levin, 2017). For example, oxygen content with depth can decline by as much as 35% between 7 and 17 m depth off the coast of California (Frieder et al., 2012), and varies over time with diurnal/diel cycling, seasonal hypoxia and El Niño–Southern Oscillation cycles (Levin et al., 2015). Organisms that experience large changes in both irradiance and oxygen include those in regions with coastal hypoxia and diel oxygen cycling (Altieri and Gedan, 2015; Tyler et al., 2009), shallow oxygen minimum and oxygen limited zones (Gilly et al., 2013; Wishner et al., 2013; Wishner et al., 2018), and shallow embayments or fjords (Hansen et al., 2002).

Understanding how the visual systems of marine organisms respond to reduced oxygen availability will provide information on constraints on habitat preference in marine organisms. Highly visual marine organisms include cephalopods (e.g. squid, octopus), arthropods (e.g. crabs, krill) and fish (McCormick and Levin, 2017). These groups support major world fisheries (FAO, 2018), and the larval stage of marine organisms is a crucial bottleneck for survival for recruitment to the fishery and reproductive population. Early life stages of arthropods, cephalopods and fish rely on vision for behaviors essential to their survival, including prey capture and predator avoidance, and as a cue for diel vertical migration (Forward, 1988; Robin et al., 2014). Vision may also be one of the sensory modalities used in larval choice of settlement site and

[1]Integrative Oceanography Division, Center for Marine Biodiversity and Conservation, Scripps Institution of Oceanography, La Jolla, CA 92093-0218, USA. [2]Department of Psychology, University of California San Diego, La Jolla, CA 92093, USA. [3]Department of Ophthalmology, University of California San Diego, La Jolla, CA 92093, USA.

*Author for correspondence (lrmccorm@ucsd.edu)

L.R.M., 0000-0001-5299-4762; L.A.L., 0000-0002-2858-8622

Received 30 January 2019; Accepted 12 April 2019

Journal of Experimental Biology (2019) 222, jeb200899. doi:10.1242/jeb.200899

List of symbols and abbreviations

CalCOFI	California Cooperative Oceanic Fisheries Investigations
ERG	electroretinogram
IR	infrared
PFD	photon flux density (μmol photons m^{-2} s^{-1})
P_{O_2}	partial pressure of oxygen
PSD	power spectral density
V_{10}	P_{O_2} with 10% of retinal function
V_{50}	P_{O_2} with 50% of retinal function
V_{90}	P_{O_2} with 90% of retinal function

detection of conspecifics in species with an adult benthic stage (Lecchini et al., 2010; Lecchini, 2011). Hypoxia is known to affect many physiological processes in marine organisms (Grieshaber et al., 1994; Wu, 2002), but to our knowledge, the effects of hypoxia on visual physiology in marine invertebrates, and specifically their larvae, have not been studied. Here, we determined how exposure to low oxygen affects (1) visual sensitivity to light, (2) the dynamic range (range of irradiance that can be detected visually) and (3) the temporal properties of vision in larvae of the market squid (*Doryteuthis opalescens*), the two-spot octopus (*Octopus bimaculatus*), the tuna crab (*Pleuroncodes planipes*) and the graceful rock crab (*Metacarcinus gracilis*). These species are representative of highly visual invertebrates of both economic and ecological interest. We hypothesized that exposure to reduced P_{O_2} in marine invertebrate larvae would decrease the magnitude of the ERG response to light stimuli, and that reduced P_{O_2} would decrease the temporal resolution of the eye.

MATERIALS AND METHODS

To investigate how retinal function changed in response to a decline in P_{O_2}, we recorded *in vivo* ERGs in tethered, intact larvae while controlling the P_{O_2} of pH-buffered seawater flowing over the animal (Fig. 1A). To control for differences in the shape of the ERG waveform across different species, we measured the size of the ERG response by integrating over the entire response. P_{O_2} in the recording chamber was measured throughout the experiments using a fiber optic probe. Partial pressure units (kPa) are presented to best represent the oxygen available for animal tissues (Seibel, 2011), but wherever reasonable, a conversion to oxygen concentration (μmol kg^{-1} O_2) was also calculated. The term 'normoxia' is used to describe surface ocean oxygen levels, approximately 100–105% saturation for the given temperature and salinity. To compare the magnitude of visual stimulation across species, we report light stimuli as a species-specific irradiance [species photon flux density (PFD; μmol photons m^{-2} s^{-1})], which is the irradiance of light at the plane of the animal's eye weighted to the spectral sensitivities for each species (Fig. S1).

Animal collection

Larvae of *Octopus bimaculatus* Verrill 1883, *Metacarcinus gracilis* (Dana 1852) and *Pleuroncodes planipes* Stimpson 1860 were obtained by conducting plankton tows at ∼30 m depth with a 325-μm mesh net in the Southern California Bight off the coast of La Jolla, CA, USA, at a recurrent market squid egg bed site (McGowan, 1954) (CA collection permit: SCP-13633; 32°51′ 30.13″N, 117°16′25.93″W) during the natural reproductive periods of each species (August 2017–April 2018). After collection, larvae of interest were kept in 0.5-liter tanks under a strict 13 h:11 h light: dark cycle, with a consistent feeding schedule [Zeigler Larval AP100 dry food (Gardners, PA, USA; crabs) or live copepods (cephalopods)], and in near-constant water temperature (16°C) prior to testing.

To obtain larvae for *Doryteuthis opalescens* (Berry 1911), divers collected freshly laid egg capsules at the same site in La Jolla (∼30 m water depth) during the full and new moon (±2 days) in January–March 2018 during the spawning period. Capsules were placed in 4-liter tanks and water chemistry was monitored throughout development until hatching (∼3–4 weeks) using Honeywell Durafet® pH sensors (Phoenix, AZ, USA) and Aanderaa oxygen optodes (model 4531; Bergen, Norway). Squid egg capsules were maintained at constant P_{O_2} (∼22 kPa/∼260 μmol kg^{-1}), temperature (11°C) and pH (∼8.2). After hatching, paralarvae were placed in smaller tanks (0.5 liters) and maintained as described for the other species.

All recently collected/hatched larvae were held for a minimum of 24 h prior to testing, and only individuals that appeared healthy upon inspection were chosen for experimentation. Only individuals of a single larval stage were used for each species (paralarvae for *D. opalescens* and *O. bimaculatus*, Stage II for *P. planipes*, and megalopae for *M. gracilis*), as different larval stages may have distinct oxygen tolerances (Yannicelli et al., 2013) and visual capabilities and/or structures (Feller et al., 2015). Here, these stages are referred to collectively as 'larvae' when individuals of multiple species are described in the text, but only individuals of the specified life stage for each species were tested. Owing to the challenge of determining sex in larvae, differences between sexes were not quantified in this study.

Electrophysiology

All procedures were in compliance with the Institutional Animal Care and Use Committee (IACUC) of the University of California San Diego, and care was taken wherever possible to reduce the stress and discomfort of the animals (e.g. transportation at a cool temperature in darkness, etc.). All experiments were conducted within 6–10 h after sunrise each day so individuals were at the same stage of circadian rhythm. All experiments were performed on dark-adapted (30 min) individuals of each species. Infrared (IR) light (940 nm) and video microscopy were used to prepare animals for recording and view animals during recording; IR light is beyond the sensitivity of most marine organisms at low intensities (Cronin and Forward, 1988; Fernandez, 1973; McCormick and Cohen, 2012). The electrophysiology recording equipment was housed in a light-tight enclosure and, with the exception of the controlled light stimuli and IR illumination for imaging, animals were kept in complete darkness for the duration of the experiment.

The recording chamber on the microscope stage was constantly perfused (∼4 ml min^{-1}) with a solution of sterile seawater (Instant Ocean, Blacksburg, VA, USA; 27 g l^{-1} of ultrapure water, salinity 33.3) and Hepes (Fisher Scientific, Hampton, NH, USA; final concentration: 20 mmol l^{-1}). The P_{O_2} of this solution was adjusted by changing the gas concentrations and flow rate of aeration (standard aquarium pump) in a solution reservoir; seawater was cooled to ecologically relevant temperatures [range of average experimental temperatures=14.1–16.4°C (*D. opalescens*); 13.9–15.8°C (*O. bimaculatus*); 13.9–15.9°C (*M. gracilis*); 13.9–15.3°C (*P. planipes*)] in an ice bath and controlled on the stage by a heater. The average pH of the solution in all experiments was 8.04±0.04. This range is within the diel variability of nearshore Southern California Bight waters; however, under natural conditions, pH would decline with decreasing oxygen in the water column (Frieder et al., 2012). Oxygen concentration was measured in the recording chamber during all experiments using a dip optical

Journal of Experimental Biology (2019) 222, jeb200899. doi:10.1242/jeb.200899

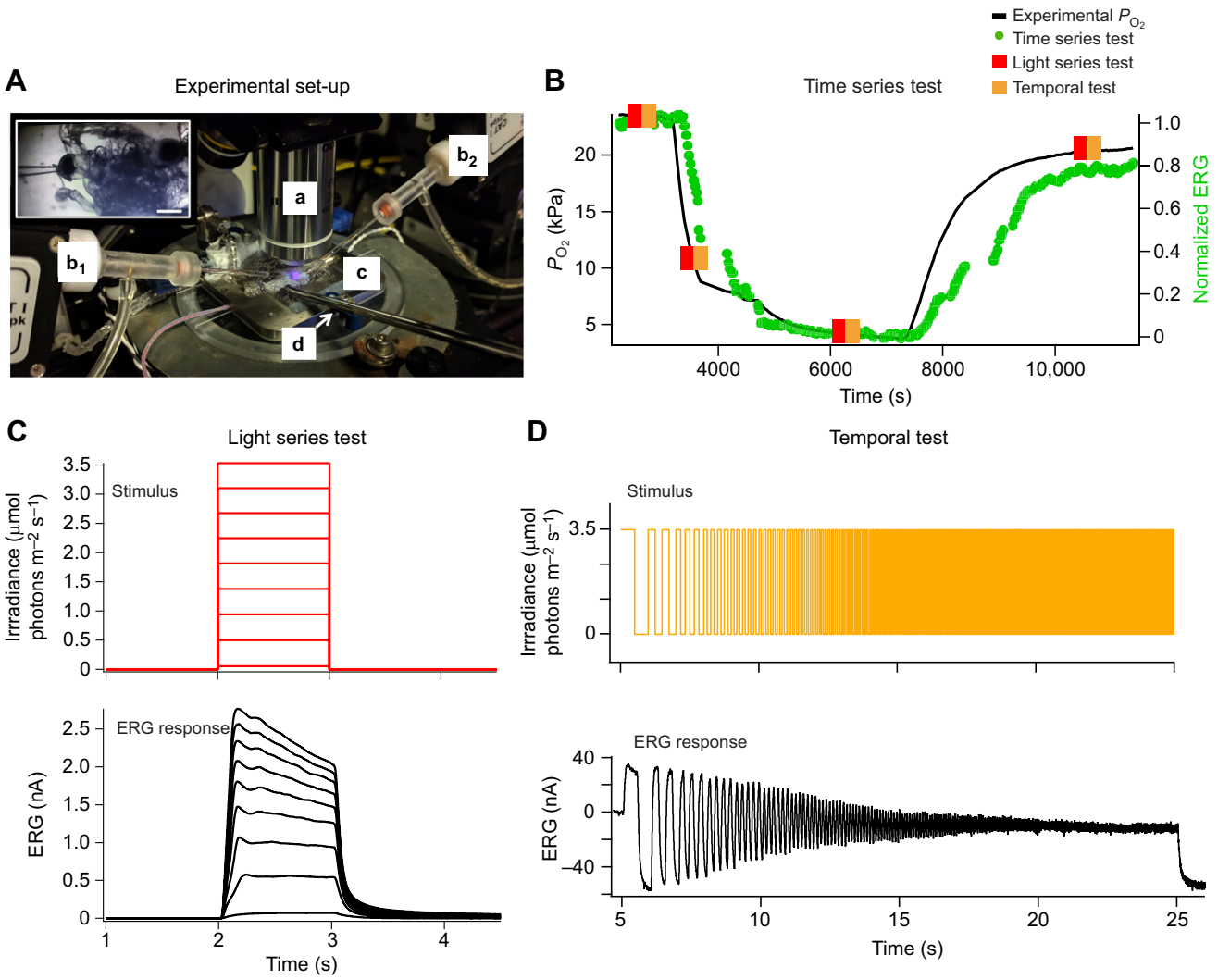

Fig. 1. Experimental design of the research project. (A) Configuration for electrophysiology experiments, showing the (a) microscope objective, (b_1/b_2) micromanipulators controlling the position of the tethered animal and the recording electrode, (c) recording stage and (d) oxygen sensor. Inset: the electrode is inserted just under the cornea of the larva (*Metacarcinus gracilis*). Scale bar: 500 µm. (B) An entire experiment consists of three visual tests. The time series test measured the electroretinogram (ERG) response (green circles) to a repeated light stimulus of a constant irradiance while the oxygen partial pressure (P_{O_2}; black line) in the recording chamber was changed gradually from normoxia to a low P_{O_2}, and then re-oxygenated to normoxia; additional experiments (described in C and D) were conducted at specific P_{O_2} values (orange and red squares). (C) The light series test consisted of nine 1-s stimuli of increasing irradiance (µmol photons m^{-2} s^{-1}; red lines) during which the change in ERG response was recorded (nA; black lines). (D) The temporal test was a chirped (1–20 Hz) square wave modulation of irradiance from darkness to a stimulus of a constant irradiance (3.5 µmol photons m^{-2} s^{-1}; orange line) used to determine the maximum frequency to which the visual system could respond (pA; black line). All example ERG responses (time series, light series and temporal test) are from a *Doryteuthis opalescens* paralarva in normoxia (P_{O_2}=21 kPa).

probe (DP-PSt7; PreSens, Regensburg, Germany; Fig. 1A). Oxygen was converted to P_{O_2} (kPa) with the 'Respirometry' package in R using the corresponding temperature and salinity from each experiment. All results are given in P_{O_2} values, with concentrations (µmol kg^{-1}) given in parentheses; all concentrations are averages of all individual trials within each species, corresponding to the temperature conditions reported above for each species.

Each larva was immobilized and its dorsal surface was attached to a borosilicate pipette using cyanoacrylate (Loctite superglue, Westlake, OH, USA) and then immediately submerged into solution on the recording chamber (using micromanipulator b_2; Fig. 1A). ERG recordings were made using a whole-cell patch clamp electrophysiology amplifier to detect and record extracellular changes in potential in the eye through a standard extracellular glass electrode. Electrodes were borosilicate pipettes pulled to a resistance of 3–6 MΩ and filled with external recording solution. Electrode tips were placed into the eye using a digital micromanipulator (micromanipulator b_1; Fig. 1A; Scientifica, Clarksburg, NJ, USA). No suction or pressure was applied to the recording electrode at any point during the experiment. The ERG signal was recorded in voltage-clamp mode using a Multiclamp 700B amplifier (Molecular Devices, San Jose, CA, USA) low-pass filtered at 4 kHz (Bessel), digitized at 20 Hz using an Instrutech ITC-18 A/D board (HEKA Elektronik, Holliston, MA, USA), and saved to a computer hard drive using the custom acquisition software writing in IgorPro (WaveMetrics, Lake Oswego, OR, USA). After obtaining an ERG recording and before beginning P_{O_2} manipulation, larvae were held in the perfusion reservoir at normoxia (equivalent to 100–105% O_2 saturation at ∼15°C and 33 salinity) to ensure there was a stable ERG response. After a stable baseline was obtained, the P_{O_2} was

decreased in the recording chamber with the addition of nitrogen gas (N_2) to the solution reservoir. After obtaining a minimum P_{O_2} value, the P_{O_2} was then increased to normoxia by adding air (21% O_2) to the reservoir (Fig. 1B).

Light stimulation

Light stimuli were generated using a collimated green super-bright T-1 3/4 package LED (525 nm; 35 nm FWHM; Thorlabs LED528EHP; Newton, NJ, USA) focused through a 2× air objective that illuminated the entire stage; stimulus irradiance was adjusted by pulse width modulation (20 kHz duty cycle) through a computer-controlled constant current driver. Irradiance (photon flux) was measured at the experimental plane with a radiometer (Thorlabs), and converted into a species-specific irradiance in units of equivalent PFD (μmol photons m^{-2} s^{-1}) for the spectral sensitivity of each species (e.g. squid PFD). Data for spectral sensitivities were obtained or modified from existing literature for the same species, or a taxonomically related species with similar life history and habitat depth: *D. opalescens* from sensitivity of *Doryteuthis pealeii* (Hubbard et al., 1959); *O. bimaculatus* from sensitivity of *O. vulgaris* (Brown and Brown, 1958); *P. planipes* (Fernandez, 1973); and *M. gracilis* from *Cancer irroratus* (Cronin and Forward, 1988). Spectral sensitivity curves were multiplied against the spectrum of the experimental light (LED) to obtain a species-specific irradiance for each species (Fig. S1). All light stimuli were presented from a dark background (no visible light), and animals were held in darkness between stimulus presentations. The term 'darkness' for this study refers to both the absence of light stimuli and the absence of environmental light within the light-tight experimental enclosure.

Three experimental irradiance manipulations were used. The time series test recorded ERG responses to a 1 s square step of light at a constant irradiance of 3.56 μmol photons m^{-2} s^{-1} repeated every 20 s, providing a nearly continuous measure of ERG response during the experimental manipulation of P_{O_2}. Two additional tests were conducted at specific oxygen conditions [normoxia (~22 kPa/~265 μmol kg^{-1}), intermediate reduction of P_{O_2} (~6.5 kPa/~95 μmol kg^{-1}) and low P_{O_2} (~3.5 kPa/~55 μmol kg^{-1}); Fig. 1B]. The light series test consisted of square step pulses of irradiance (1 s light stimulus every 7 s) increasing from dim light to bright light (0.056–3.53 μmol photons m^{-2} s^{-1}) at nine equally spaced irradiance increments, repeated three times with 20 s in between each series at each oxygen condition (Fig. 1C). The temporal test consisted of a chirped (1–20 Hz) square wave modulated between darkness and an irradiance of 3.26 μmol photons m^{-2} s^{-1} (Fig. 1D). Time series and light series tests were completed on larvae of all four species. The temporal test was completed on *D. opalescens* paralarvae and *P. planipes* larvae due to the lack of availability of *O. bimaculatus* paralarvae or *M. gracilis* megalopae at the time of experiments. All oxygen values were measured directly on the stage throughout visual tests. Experiments were conducted *in vivo*, with 100% survival of all larvae throughout the duration of the experiment.

Analysis of results

All electrophysiology data were analyzed using the software IgorPro (WaveMetrics). All waves were down-sampled to 2 kHz, digitally filtered with a binomial smoothing algorithm (IgorPro) with a corresponding Gaussian filter cut-off frequency of 40 Hz, and digitally notch filtered (60 Hz) before analysis. For all square waves, the amplitude of the response and the integrated area under the waveform were calculated. Within a species there was no difference in results when the measurement of the amplitude or the area was used, but because of the differences in waveform shapes between species, the integrated measurement was used for all final results.

For time series data, all measurements were normalized to the average of the ERG response in normoxia during the 5 min prior to the initiation of oxygen decline. Each normalized ERG measurement was matched to the corresponding oxygen measurement, and ERG responses were averaged over every minute to smooth the data. Oxygen metrics for retinal function, V_{90}, V_{50} and V_{10}, defined as the P_{O_2} where there was 90%, 50% and 10% retinal function, respectively, were calculated for each trial and averaged across individuals. Statistical differences between metrics (V_{90}, V_{50} and V_{10}) were determined using Kruskal–Wallis one-way ANOVAs within each species (d.f.=2 for *D. opalescens*, *O. bimaculatus* and *M. gracilis*; d.f.=1 for *P. planipes*). Pairwise differences between metrics (e.g. V_{90} versus V_{50}, etc.) were determined using Dunn's test with Bonferroni correction for multiple comparisons (d.f.=2 for *D. opalescens*, *O. bimaculatus* and *M. gracilis*; d.f.=1 for *P. planipes*).

For light series data, three repeated tests were averaged at each oxygen condition. Both the amplitude of and area under the response waveform were calculated, and the integrated area was used for final analysis as explained for the time series data. ERG responses to stimuli at each irradiance were normalized to the maximum response (during normoxia at the highest irradiance). Response–irradiance curves were fit with a Hill equation for the averages of each species, as is often used to describe visual response–irradiance functions (Shapley and Enroth-Cugell, 1984; Oesch and Diamond, 2011). Within each species, Kruskal–Wallis one-way ANOVAs were conducted to determine differences between ERG responses at each oxygen condition (normoxia, ~22 kPa/~265 μmol kg^{-1}; intermediate reduction of P_{O_2}, ~6.5 kPa/~95 μmol kg^{-1}; and low P_{O_2}, ~3.5 kPa/~55 μmol kg^{-1}) at each irradiance (d.f.=2; Table S1). To determine whether changes in retinal function in different oxygen conditions were consistent across irradiance (i.e. whether the shape of the response changed with oxygen condition), values were also normalized to the maximum value (ERG response at highest irradiance) within each oxygen condition. Oxygen values presented are averages from all trials within each species.

For temporal response analysis, three presentations at each oxygen concentration were averaged. In some cases, low oxygen reduced the amplitude of the response so that it became indistinguishable from the baseline noise. Therefore, only data where the light response was greater than 2 standard deviations of the baseline noise was used. Power spectral densities (PSDs) were calculated using the fast Fourier transform (window size=4000). The resulting PSD was normalized to the value at 1 Hz and converted to gain (dB). Results were analyzed for significance using a Kruskal–Wallis one-way ANOVA on the cut-off frequency (–6 dB) at each oxygen condition for each of the two species (*D. opalescens* and *P. planipes*) tested. Oxygen values (in partial pressure and concentration) presented are averages from all trials within each species.

The potential for loss of retinal function from P_{O_2} in the environment in the Southern California Bight was calculated using the physiological threshold data collected in this study and the oxygen concentration data collected via CTD (conductivity–temperature–depth) casts made during California Cooperative Oceanic Fisheries Investigations (CalCOFI) cruises. Data from springtime (March–May) cruises conducted between 2005 and 2017 were downloaded from the CalCOFI website (calcofi.org) and casts closest to the animal collection site for these experiments (line 93.3 station 26.7 and 28) between 2005 and 2017 were averaged.

Journal of Experimental Biology (2019) 222, jeb200899. doi:10.1242/jeb.200899

Oxygen data from these casts were converted from concentration (μmol kg^{-1}) to P_{O_2} (kPa) units using the R package 'AquaEnv' and code from Hofmann et al. (2011). ERG response data from physiology experiments and the corresponding P_{O_2} were fit with the best-fit model for each species (linear for *D. opalescens* and *M. gracilis* and nonlinear for *O. bimaculatus* and *P. planipes*) to calculate the predicted retinal function at each 1-m depth bin.

Images for each species were inspired by photographs (*D. opalescens* and *O. bimaculatus*) or existing drawings of larval stages [*P. planipes* (Boyd, 1960) and *M. gracilis* (Ally, 1975)].

RESULTS

Sensitivity to light

During a continuous decline in P_{O_2} from 22 kPa (280 μmol kg^{-1} O_2=normoxia) to ∼3 kPa (∼45 μmol kg^{-1}), the amplitude of the ERG to a 1 s square step pulse of light from darkness to a constant irradiance of 3.56 μmol photons m^{-2} s^{-1} decreased by 60–100% relative to responses in normoxia in all species ('time series test'; Fig. 1B). The magnitude of retinal impairment and the P_{O_2} at which the decline began differed among species (Fig. 2). The calculated oxygen metrics for retinal function show declines across all species as P_{O_2} decreases, with significant differences between V_{90}, V_{50} and V_{10} within a species in *D. opalescens* (P=0.012) and *M. gracilis* (P=0.006), but not in *O. bimaculatus* (P=0.156) or *P. planipes* (P=0.655, Kruskal–Wallis tests; Fig. 2).

Surprisingly, retinal function (V_{90}) began declining at relatively high P_{O_2} (only 1–2 kPa/20–30 μmol kg^{-1} below oxygen saturation) in *D. opalescens* (V_{90}=22.2 kPa/258 μmol kg^{-1}) and *M. gracilis* (V_{90}=19.4 kPa/229 μmol kg^{-1}). In contrast, oxygen thresholds for vision in *O. bimaculatus* (V_{90}=11.5 kPa/133 μmol kg^{-1}) and *P. planipes* (V_{90}=5.7 kPa/68 μmol kg^{-1}) were at lower P_{O_2} values. Retinal function continued to decline with further reductions of oxygen in *D. opalescens*, *O. bimaculatus* and *M. gracilis*, and the P_{O_2} where only 50% ERG function remained (V_{50}) for each species was 13 kPa (151 μmol kg^{-1}), 7.2 kPa (85 μmol kg^{-1}) and 10.2 kPa (121 μmol kg^{-1}), respectively (Fig. 2). In all cases, the ERG response returned to at least 50% of the maximum response (relative to the initial responses in normoxia) after re-oxygenation of the solution (Fig. 3), indicating the decline in ERG response during exposure to reduced P_{O_2} was not from the death of the retinal tissue.

Dynamic range

To determine whether the oxygen effects were dependent on light level, we presented light steps over a range of irradiance from 0.056 to 3.53 μmol photons m^{-2} s^{-1} at three different oxygen conditions

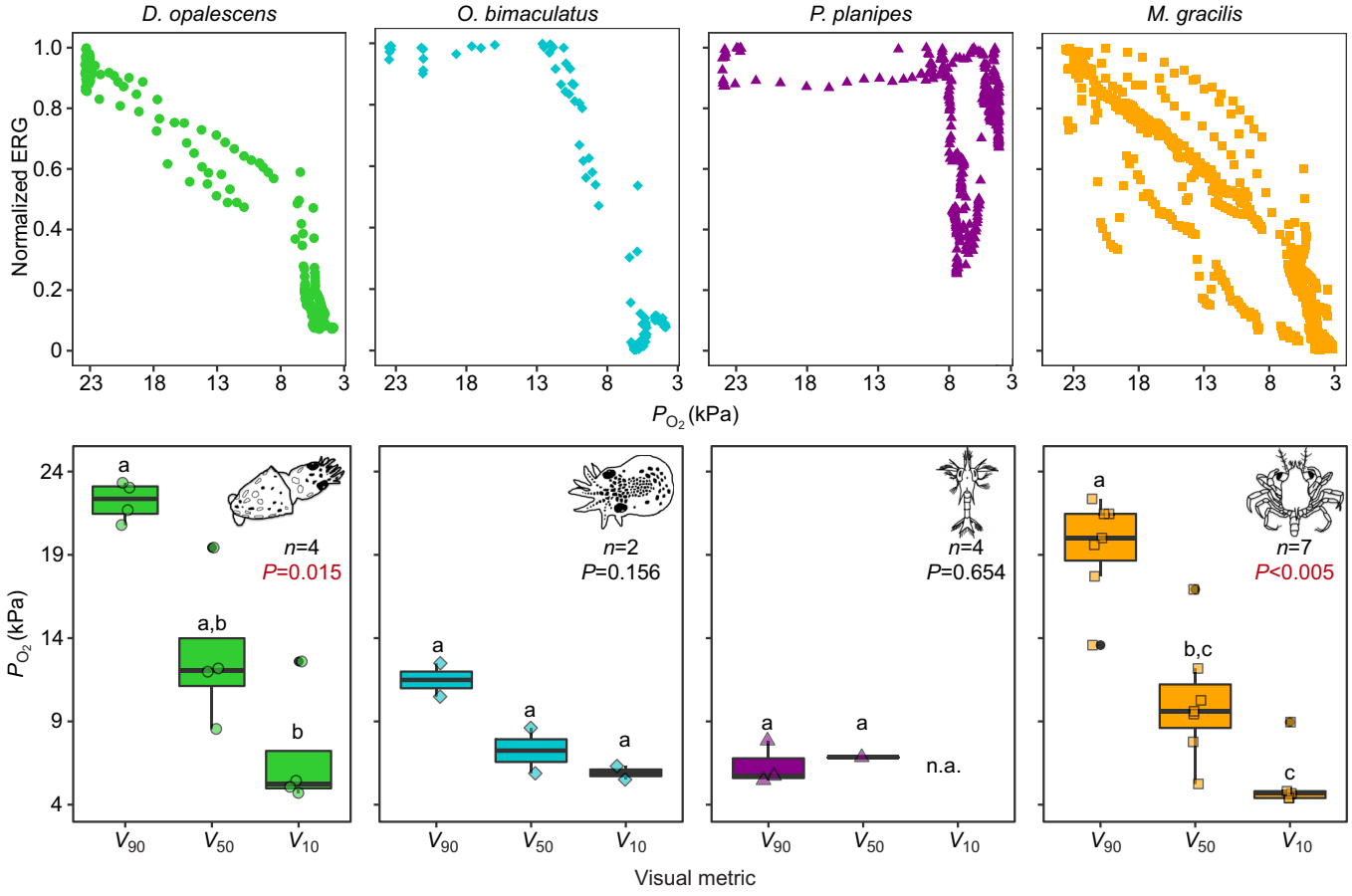

Fig. 2. Quantifying the decline in retinal function from exposure to reduced P_{O_2} in marine invertebrate larvae. Top row: change in ERG response (normalized to the average at normoxia oxygen exposure) to a 1-s light stimulus (3.56 μmol photons m^{-2} s^{-1}) every 20 s over a decline in oxygen partial pressure (kPa) for the market squid, *Doryteuthis opalescens* (green circles), the two-spot octopus, *Octopus bimaculatus* (teal diamonds), the tuna crab, *Pleuroncodes planipes* (magenta triangles), and the graceful rock crab, *Metacarcinus gracilis* (orange squares). Bottom row: visual metrics showing the partial pressure of oxygen where there is 90% (V_{90}), 50% (V_{50}) and 10% (V_{10}) of retinal function (with respect to ERG responses in normoxia) for each of the four species. The *P*-values indicate results of a Kruskal–Wallis one-way ANOVA across metrics for each species; different lowercase letters indicate significant pairwise differences (Dunn's test) between metrics (within a species). Boxes show the median (bold center line) and first and third quartiles of all individuals tested within a species; error bars show maximum/minimum values within 1.5× the inner quartile range (IQR=third quartile–first quartile), with all data points used in the analyses overlaid.

Journal of Experimental Biology (2019) 222, jeb200899. doi:10.1242/jeb.200899

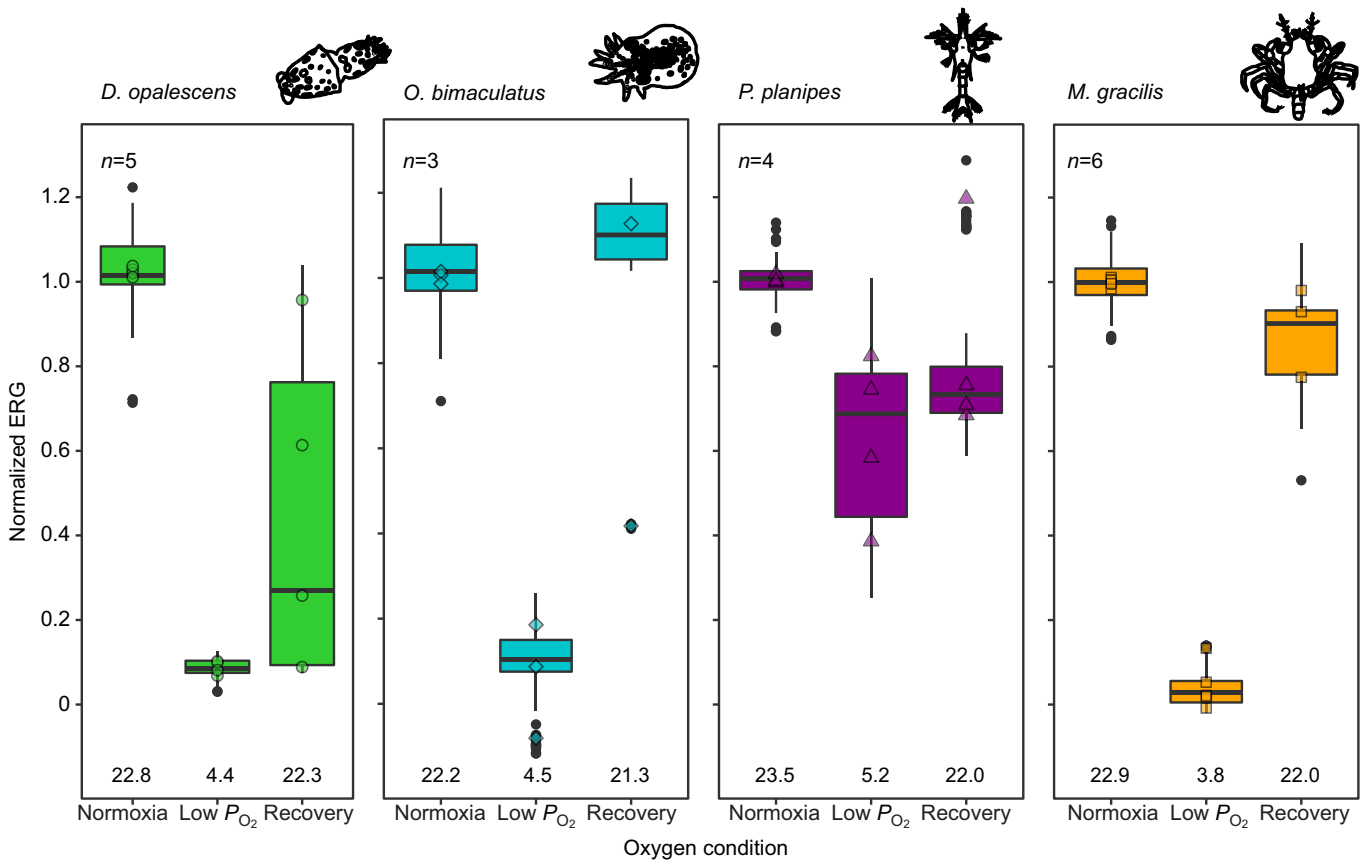

Fig. 3. Recovery of retinal function after exposure to reduced P_{O_2}. Average ERG responses (all normalized to ERG response in normoxia) during initial exposure to normoxia, low P_{O_2} and after re-oxygenation of the solution to recovery normoxia (recovery) in larvae of *D. opalescens* (green), *O. bimaculatus* (teal), *P. planipes* (magenta) and *M. gracilis* (orange). Average P_{O_2} for each condition is displayed in kPa; boxes show the median (bold line) bounded by first and third quartiles and error bars show maximum/minimum values within 1.5× the IQR, with outliers as black circles. All data used for the analyses are overlaid.

(normoxia, intermediate reduced P_{O_2} and low P_{O_2}; 'light series test'; Fig. 1C). There was a decrease in ERG amplitude across all irradiances tested in all species as P_{O_2} decreased (Fig. 4), similar to what was observed in the first experiment, indicating that declines in ERG responses observed in low P_{O_2} were not irradiance-dependent (Fig. 4A,C,E,G). At each irradiance tested, ERG responses were significantly different between the ERG response at normoxia, intermediate reduced P_{O_2} and low P_{O_2} ($P<0.05$, Kruskal–Wallis tests; Fig. 4, Table S1), with the exception of the lowest irradiance (0.056 µmol photons m^{-2} s^{-1}) in larvae of *D. opalescens*, *O. bimaculatus* and *P. planipes* ($P=0.246$, 0.301 and 0.105, respectively). To quantify the response–irradiance relationship (ERG response at each irradiance), ERG responses at each oxygen condition were fit with a Hill equation (Fig. 4A,C,E,G). To examine how the shape of the response–irradiance relationship was influenced by oxygen, we scaled the responses to the maximum ERG response within each oxygen condition (Fig. 5). Small changes in the shape of the response–irradiance relationship were seen in the cephalopods (*D. opalescens* and *O. bimaculatus*), but differences in the ERG response across oxygen conditions at each irradiance were not statistically significant in any species, indicating the response–irradiance relationships were stable at different oxygen conditions ($P>0.05$, Kruskal–Wallis tests; Table S1).

Temporal resolution

To determine how P_{O_2} affects the temporal properties of the larval ERG response, we presented square wave linear chirp stimuli (frequency modulated between 1 and 20 Hz) between darkness and a constant irradiance of 3.56 µmol photons m^{-2} s^{-1} in larvae of *D. opalescens* and *P. planipes* ('temporal test'; Fig. 1D) and measured the corresponding ERG response. With this recording of ERG response to flashes of light at multiple frequencies, we computed the PSD to determine the power of the visual signal at each frequency. As expected, there was a decline in the power of the response as frequency increased, indicative of the natural temporal resolution limit for the species (Fig. 6). We quantified the temporal resolution using a cut-off frequency (frequency at which power drops below −6 dB). During exposure to low P_{O_2}, we observed a steeper decline in the power of the response in larval *D. opalescens*, with a cut-off frequency decreasing from 4.6 Hz at normoxia (23.1 kPa) to 2.8 Hz at low P_{O_2} (3.8 kPa; $P=0.009$, Kruskal–Wallis test; Fig. 6). No significant change in temporal resolution was observed with a change of P_{O_2} in *P. planipes* (7.5 Hz at 23.4 kPa to 6.8 Hz at 3.6 kPa; $P=0.755$, Kruskal–Wallis test; Fig. 6). This indicates that the temporal resolution of vision in paralarvae of *D. opalescens* was reduced when exposed to low P_{O_2}, but that larvae of *P. planipes* were not significantly affected within the range of P_{O_2} tested here.

DISCUSSION

Based on studies in terrestrial vertebrates, we expected that large decreases in oxygen would reduce ERG responses; however, for most marine species, the magnitude of the reduction in oxygen needed to impact retinal function is unknown. It is also unknown

Journal of Experimental Biology (2019) 222, jeb200899. doi:10.1242/jeb.200899

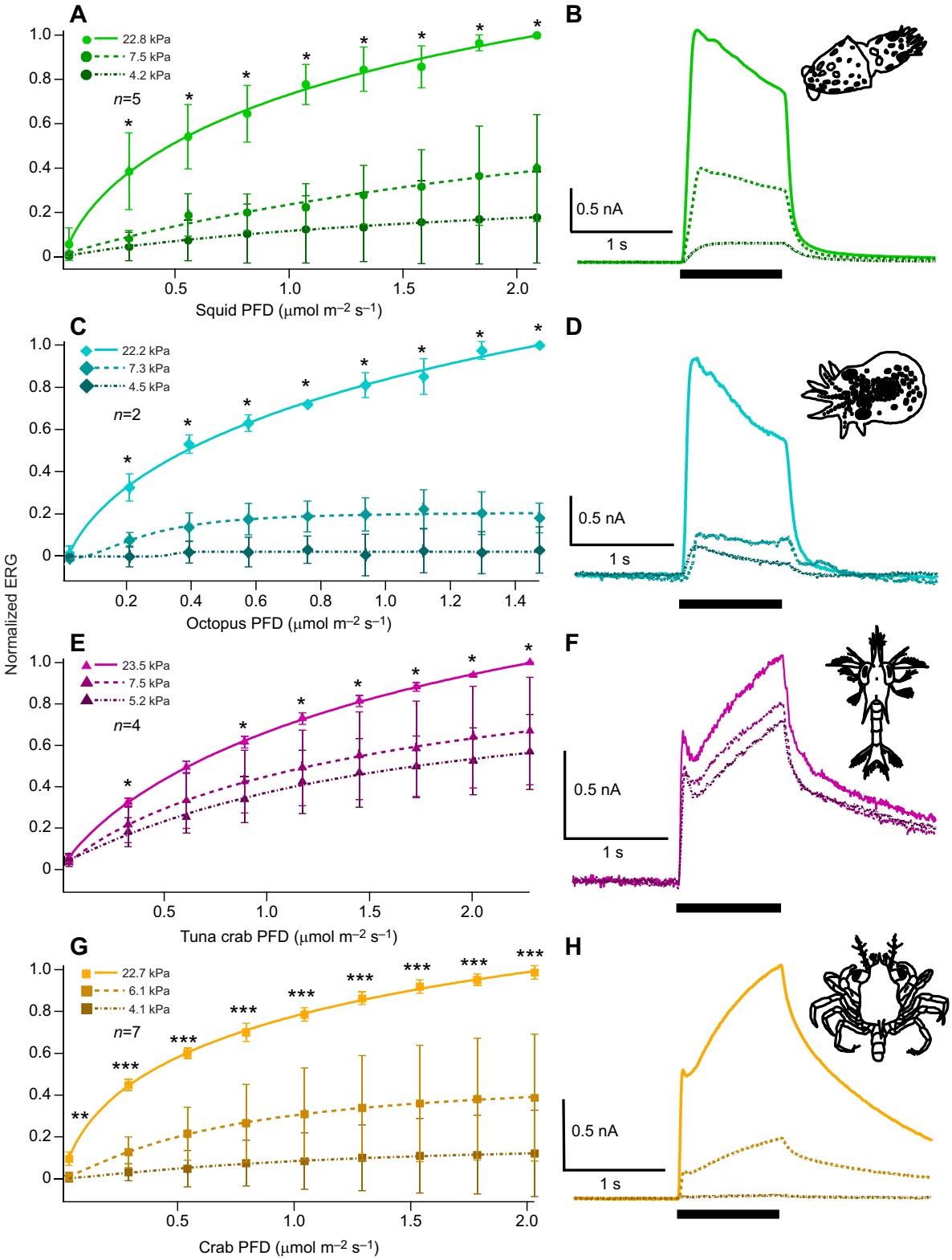

Fig. 4. Effects of reduced P_{O_2} on retinal responses at a range of irradiances. ERG response to oxygen tested at multiple irradiances in larvae of (A,B) *D. opalescens*, (C,D) *O. bimaculatus*, (E,F) *P. planipes* and (G,H) *M. gracilis*. (A,C,E,G) Response–irradiance curves show the ERG response (normalized to the maximum response in normoxia) to stimuli of nine different irradiance levels (PFD) for *D. opalescens* (green circles), *O. bimaculatus* (teal diamonds), *P. planipes* (magenta triangles) and *M. gracilis* (orange squares) during exposure to normoxia (22.3–23.5 kPa), intermediate reduced P_{O_2} (6.1–7.5 kPa) and low P_{O_2} (4.1–5.2 kPa) fit with a Hill equation (solid, dashed and dash–dotted lines, respectively). Differences between ERG responses at each oxygen condition within each of the irradiances were determined using Kruskal–Wallis one-way ANOVAs; asterisks indicate significance (*P<0.05; **P<0.01; ***P<0.001). Error bars show means±s.d. (B,D,F,H) Representative ERG responses to a 1-s stimulus at the maximum irradiance from a single larva. Horizontal scale bars (for all) indicate 1 s; vertical bars are 0.5 nA in B and H and 0.05 nA in D and F; thick black bar indicates the duration of the light stimulus. Color shades and lines follow oxygen levels in A, C, E and G.

Journal of Experimental Biology (2019) 222, jeb200899. doi:10.1242/jeb.200899

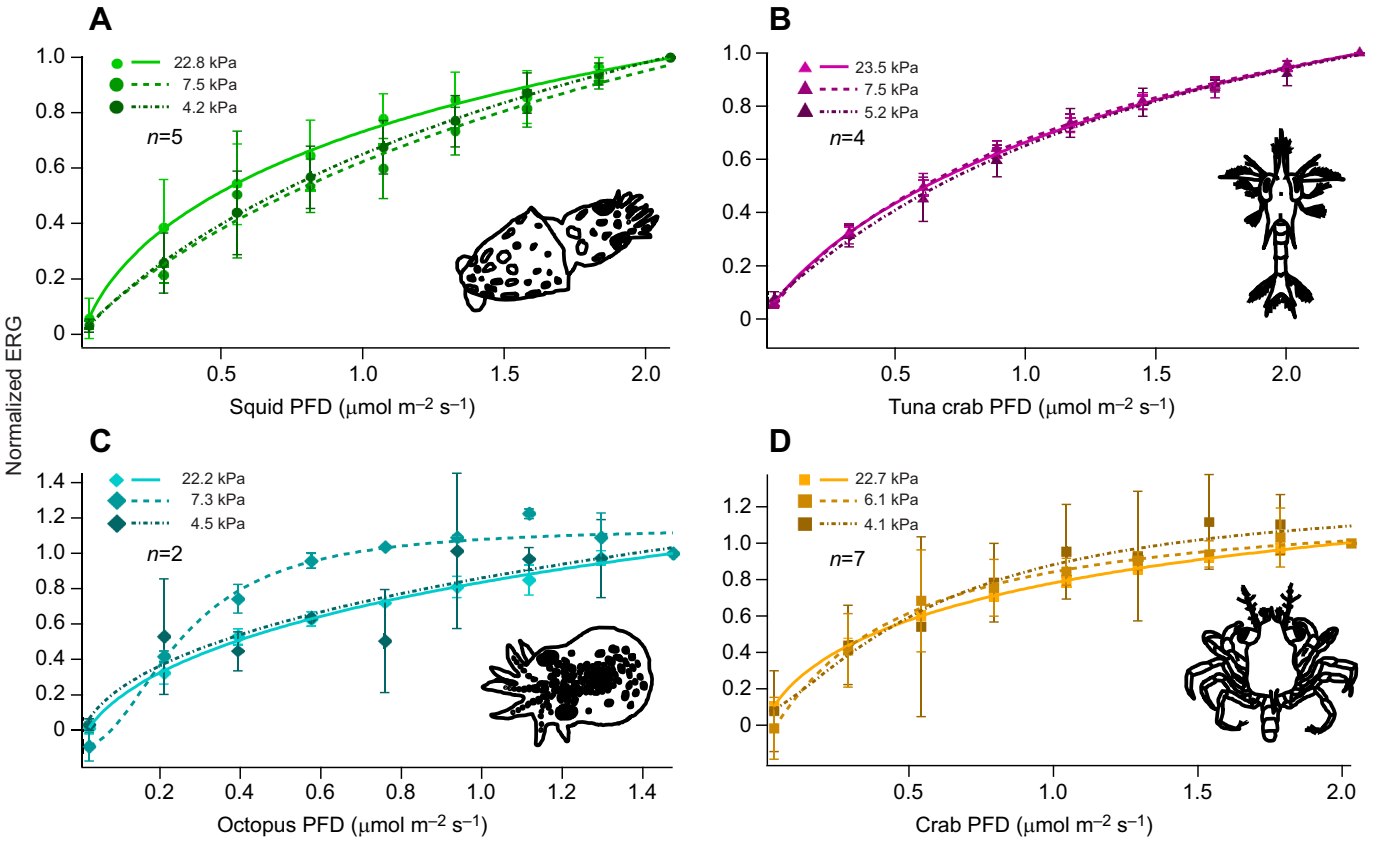

Fig. 5. Oxygen effects on response–irradiance relationships. Differences in the shape of ERG responses to increasing irradiance at each oxygen condition. Response–irradiance curves (normalized to the maximum response in each oxygen condition) show the shape of the visual response to stimuli of nine different irradiances in larvae of (A) *D. opalescens* (green circles), (B) *P. planipes* (magenta triangles), (C) *O. bimaculatus* (teal diamonds) and (D) *M. gracilis* (orange squares) during exposure to normoxia (22.3–23.5 kPa), intermediate reduced P_{O_2} (6.1–7.5 kPa) and low P_{O_2} (4.1–5.2 kPa). ERG responses during exposure to each oxygen condition are fit with a Hill equation (solid, dashed and dash–dotted lines, respectively). Error bars indicate means±s.d.

whether the decline in retinal function occurs at some threshold oxygen concentration or more continuously as oxygen is decreased below some critical threshold. To our knowledge, no direct comparisons of oxygen effects on visual physiology between different groups of marine invertebrates exist. These results demonstrated major retinal impairment in three species of marine invertebrate larvae after exposure to surprisingly minor amounts of oxygen decline (decreases of 1–2 kPa/20–30 μmol kg^{-1} from oxygen saturation). Interestingly, there were large differences in visual sensitivity to low P_{O_2} among species, with almost 100% loss of retinal function in larvae of *D. opalescens*, *O. bimaculatus* and *M. gracilis* at low P_{O_2} (~3 kPa), whereas retinal function in larvae of *P. planipes* was relatively unaffected (i.e. ERG responses never declined enough to define a V_{10} within the range of P_{O_2} tested). Additionally, during exposure to a decline in P_{O_2}, the retinal responses decreased continuously in *D. opalescens* paralarvae and *M. gracilis* megalopae, whereas *O. bimaculatus* paralarvae and *P. planipes* larvae were able to maintain ≥90% retinal responses until ~11 and ~8 kPa, respectively, before ERG responses began showing the effects of decreased oxygen availability (Fig. 2).

The two species tested for temporal resolution also had very different responses to exposure to low P_{O_2}. Paralarvae of *D. opalescens* showed a strong decrease in the power of the retinal response at higher frequencies during exposure to low P_{O_2}, whereas the larvae of *P. planipes* showed very little change in temporal resolution. These differences in retinal responses across species are likely due to different metabolic tolerances to low oxygen; however, data for critical oxygen thresholds for metabolism (as in Seibel et al., 2016) do not yet exist for larvae in these species. In addition, the decrease in retinal function after only minor declines in P_{O_2} suggest that oxygen effects on vision may be an important sublethal physiological effect of low oxygen that may not be captured completely by a metric such as the critical oxygen thresholds for metabolism.

The declines in retinal responses for these invertebrate larvae during exposure to reduced oxygen are comparable to what is reported for terrestrial mammals. For example, the ERG response in cats began decreasing almost immediately after a decline in oxygen started, at P_{O_2} values similar to what would be experienced if a human were to drive from sea level to approximately 2000 m elevation (e.g. Lake Tahoe in California) (Linsenmeier et al., 1983; Steinberg, 1987). The effects of oxygen on the visual system of the cat were noted to occur at P_{O_2} values much greater than when effects would be observed in other neural circuits (Linsenmeier et al., 1983). The P_{O_2} values that cause a reduction in marine invertebrate larval vision are well within the range of variability they experience in their natural environment. For example, the average daily range of oxygen (caused by both biological and physical forcing) in coastal areas of the Southern California Bight is ~63 μmol kg^{-1} (~4 kPa at 15°C) at 7 m depth (Frieder et al., 2012); our results suggest that this magnitude of variability (ΔP_{O_2}=4 kPa), even at high P_{O_2} (21–17 kPa), could cause a 10–20% decrease in retinal function in larvae of *D. opalescens* and *M. gracilis* (Fig. 2) if they did not move upward to better-oxygenated waters. In addition, using the

Journal of Experimental Biology (2019) 222, jeb200899. doi:10.1242/jeb.200899

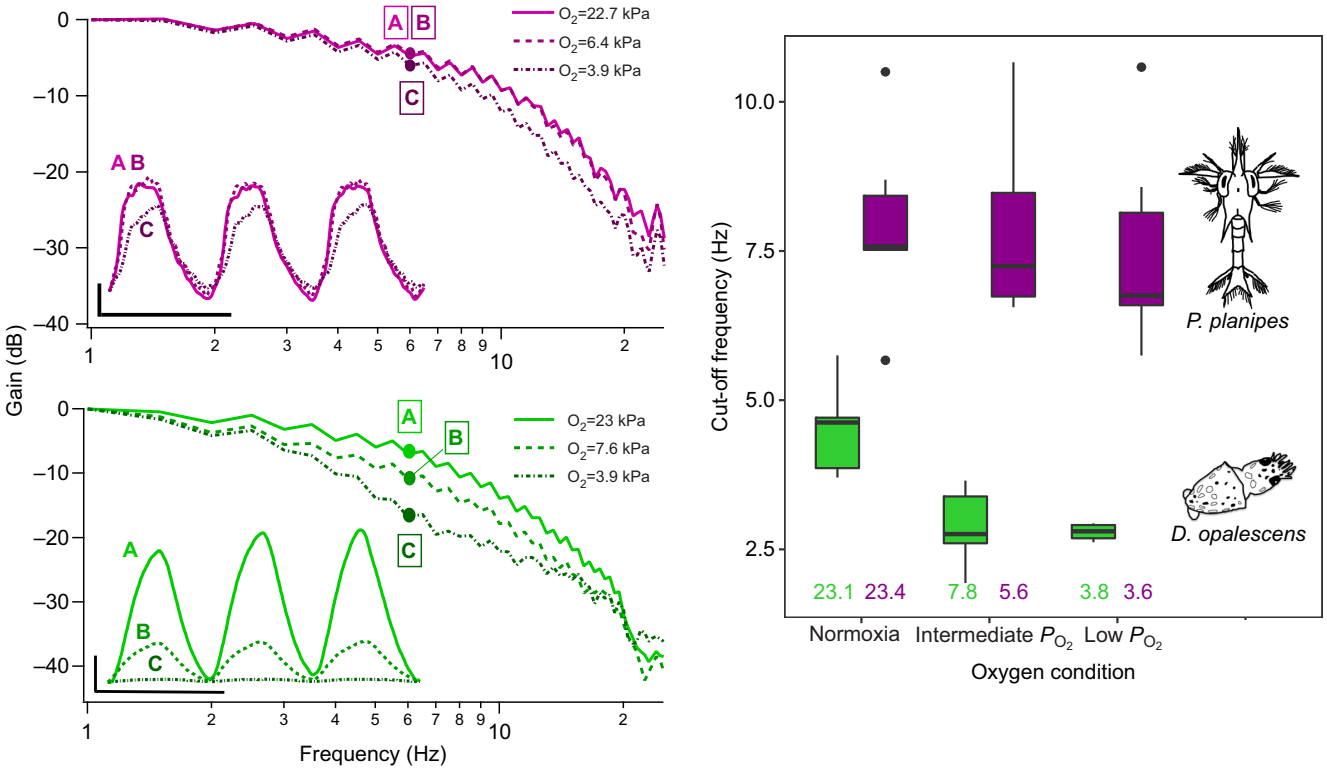

Fig. 6. Effects of reduced P_{O_2} on the temporal resolution of vision. Left: power spectral density (PSD) curves (normalized to value at 1 Hz) showing the power of the temporal response over stimulus frequencies from 1 to 20 Hz at three decreasing oxygen conditions (solid, dashed and dash–dotted lines, respectively) in an example larva of *P. planipes* (top; magenta) and an example paralarva of *D. opalescens* (bottom; green). Inset: example traces for each species showing the ERG response at the marked frequency (6 Hz) for responses in normoxia (A), intermediate reduction of P_{O_2} (B) and low P_{O_2} (C), respectively. Horizontal scale bar represents 0.25 s and the vertical scale bar represents 20 pA (top) or 100 pA (bottom). Right: calculated cut-off frequencies (–6 dB change in PSD) for each oxygen condition (values in figures on left) for all individuals of both *D. opalescens* (green; *n*=6) and *P. planipes* (magenta; *n*=6). The average P_{O_2} for each condition (kPa) is displayed for both *D. opalescens* (green) and *P. planipes* (magenta). Boxes show the median (bold center line) and first and third quartiles; whiskers show 1.5× the IQR, with outliers as black circles.

visual sensitivity of each species to P_{O_2} reported above (e.g. Fig. 2), we calculated the decrease in retinal function with depth under present-day (2005–2017) average springtime ocean oxygen conditions in the Southern California Bight. The decline in P_{O_2} alone from 0 to 30 m depth would decrease retinal function by 15–59% in larvae of *D. opalescens*, *M. gracilis*, *O. bimaculatus* and *P. planipes* in coastal Southern California (Fig. 7), even without including the effects of decreasing irradiance on the ERG response. Such changes in oxygen levels could significantly reduce larval fitness through loss of retinal function; however, the manifestation of the physiological impairment in visual behavior is unknown.

Many marine larvae remain at depth during the day to avoid visual predation, often at the depth near their threshold for light detection; they then migrate vertically to near-surface waters at night when predation pressure is reduced (diel vertical migration) (Forward, 1988; Sulkin, 1984; Zeidberg and Hamner, 2002). In all species, but especially in larvae of *D. opalescens*, *O. bimaculatus* and *M. gracilis*, retinal sensitivity to light declined during exposure to reduced oxygen (Fig. 2). Larvae of *O. bimaculatus* also experienced a decline in the range of irradiance that was physiologically detected, indicating that the sensitivity to changes in light irradiance (contrast) will be reduced during exposure to reduced P_{O_2}. For example, the shadow of a predator may become undetectable. Marine larvae require sufficiently high temporal resolution (the ability to distinguish between stimuli varying in time) to detect and appropriately respond to predators or prey (Frank, 1999). The decline in temporal resolution under reduced P_{O_2} in larvae of *D. opalescens* would reduce the ability to detect high-frequency movements, such as the burst-swimming pattern of the copepods they feed on. Decreased light sensitivity and temporal resolution induced by low oxygen may introduce a greater risk for predation, increase vulnerability to starvation (if prey detection is reduced) and/or potentially weaken detection of the light cue for vertical migration entirely if the decrease in retinal response is sufficient to change visual behaviors. All individuals recovered some level of retinal function with re-oxygenation of the solution after the acute exposure time of the experiments (~30 min at reduced oxygen; Fig. 3), indicating that the retinal response may recover during the time required for a small larva (~1.5–3 mm) to swim a few meters.

These data also have important practical implications for researchers studying these organisms in a laboratory setting. The significant changes in retinal function after even small depletions in oxygen availability for some species suggest that it is important to monitor and maintain appropriate oxygen levels during *in vitro* and *in vivo* experiments.

Knowledge of how the retinal function of marine invertebrate species changes during exposure to reduced P_{O_2} may help define species-specific vulnerabilities and resilience to future oxygen loss in the ocean. Globally, oxygen declines have resulted from warming (Schmidtko et al., 2017) and from nutrient and organic loading (Breitburg et al., 2018), and these losses can be exacerbated in areas with naturally occurring coastal hypoxia and upwelling (Altieri and Gedan, 2015; Levin and Breitburg, 2015). Given the apparent high

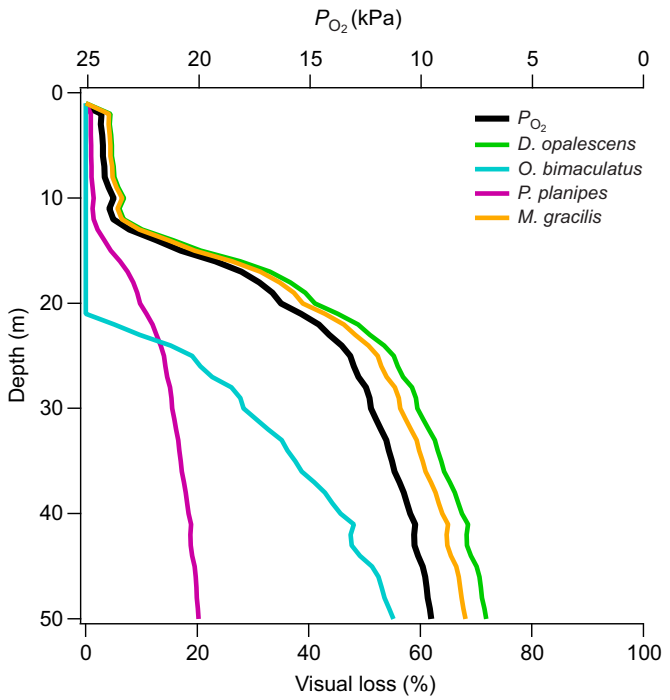

Fig. 7. Loss in retinal function in marine larvae from decreasing P_{O_2} with depth. Using physiological data from Fig. 2, the predicted change in retinal function (percent visual loss) is shown for an average springtime (March–May; data from 2005 to 2017) profile of P_{O_2} (black line) with depth in the Southern California Bight for *D. opalescens* (green line), *O. bimaculatus* (teal line), *P. planipes* (magenta line) and *M. gracilis* (orange line).

visual sensitivity and species-specificity of visual tolerance to low oxygen, documenting how larval (and adult) vulnerabilities to low oxygen are manifested in visual behaviors and ecology will be important for predicting responses to global and local declines in ocean oxygen.

Acknowledgements
We thank P. Zerofski for help with larval collections, and J. H. Cohen, D. Deheyn, T. Martz, F. Powell and M. Tresguerres for comments on data and analysis, as well as two anonymous reviewers, who helped improve the manuscript.

Competing interests
The authors declare no competing or financial interests.

Author contributions
Conceptualization: L.R.M.; Methodology: L.R.M., N.W.O.; Software: L.R.M., N.W.O.; Validation: L.R.M., N.W.O.; Formal analysis: L.R.M.; Investigation: L.R.M.; Resources: L.R.M., L.A.L., N.W.O.; Writing - original draft: L.R.M.; Writing - review & editing: L.R.M., L.A.L., N.W.O.; Visualization: L.R.M.; Supervision: L.A.L., N.W.O.; Funding acquisition: L.R.M., L.A.L., N.W.O.

Funding
This research was supported by a Charles H. Stout Foundation grant, a Frontiers of Innovation Scholars Program grant from the University of California San Diego, and the Scripps Institution of Oceanography education office for support to L.R.M., a National Science Foundation Graduate Research Fellowship grant DGE-1144086 to L.R.M., and a National Science Foundation grant OCE-1829623 to L.A.L. and N.W.O.

Supplementary information
Supplementary information available online at
http://jeb.biologists.org/lookup/doi/10.1242/jeb.200899.supplemental

References
Ally, J. R. R. (1975). A description of the laboratory-reared larvae of *Cancer gracilis* Dana, 1852 (Decapoda, Brachyura). *Crustaceana* **28**, 231-246. doi:10.1163/156854075x00496

Altieri, A. H. and Gedan, K. B. (2015). Climate change and dead zones. *Glob. Chang. Biol.* **21**, 1395-1406. doi:10.1111/gcb.12754

Ames, A. I. (2000). CNS energy metabolism as related to function. *Brain Res. Rev.* **34**, 42-68. doi:10.1016/S0165-0173(00)00038-2

Boyd, C. M. (1960). The larval stages of *Pleuroncodes planipes* Stimson (Crustacea, Decapoda, Galatheidae). *Biol. Bull.* **118**, 17-30. doi:10.2307/1539052

Breitburg, D., Levin, L. A., Oschlies, A., Grégoire, M., Chavez, F. P., Conley, D. J., Garçon, V., Gilbert, D., Gutiérrez, D., Isensee, K. et al. (2018). Declining oxygen in the global ocean and coastal waters. *Science* **359**, 7240. doi:10.1126/science.aam7240

Brown, K. T. (1968). The electroretinogram: its components and their origins. *Vision Res.* **8**, 633-677. doi:10.1016/0042-6989(68)90041-2

Brown, P. K. Brown, P. S. (1958). Visual pigments of the octopus and cuttlefish. *Nature* **182**, 1288-1290. doi:10.1038/1821288a0

Chen, D.-M. and Stark, W. S. (1994). Electroretinographic analysis of ultraviolet sensitivity in juvenile and adult goldfish retinas. *Vision Res.* **34**, 2941-2944. doi:10.1016/0042-6989(94)90265-8

Chrispell, J. D., Rebrik, T. I. and Weiss, E. R. (2015). Electroretinogram analysis of the visual response in zebrafish larvae. *J. Vis. Exp.* 97, e52662 doi:10.3791/52662

Cohen, J. H., Berge, J., Moline, M. A., Sørensen, A. J., Last, K., Falk-Petersen, S., Renaud, P. E., Leu, E. S., Grenvald, J., Cottier, F. et al. (2015). Is ambient light during the high Arctic polar night sufficient to act as a visual cue for zooplankton? *PLoS ONE* **10**, e0126247. doi:10.1371/journal.pone.0126247

Cronin, T. W. and Forward, R. B. (1988). The visual pigments of crabs: I. Spectral characteristics. *J. Comp. Physiol. A* **162**, 463-478. doi:10.1007/BF00612512

FAO (2018). *The State of World Fisheries and Agriculture 2018-Meeting the Sustainable Development Goals*. Rome: FAO.

Feller, K. D., Cohen, J. H. and Cronin, T. W. (2015). Seeing double: visual physiology of double-retina eye ontogeny in stomatopod crustaceans. *J. Comp. Physiol. A* **201**, 331-339. doi:10.1007/s00359-014-0967-2

Fernandez, H. R. (1973). Spectral sensitivity and visual pigment of the compound eye of the galatheid crab *Pleuroncodes planipes*. *Mar. Biol.* **20**, 148-153. doi:10.1007/BF00351453

Forward, R. B. (1988). Diel vertical migration: zooplankton photobiology and behavior. *Oceanogr. Mar. Biol.* **26**, 361-393.

Fowler, B., Banner, J. and Pogue, J. (1993). The slowing of visual processing by hypoxia. *Ergonomics* **36**, 727-735. doi:10.1080/00140139308967933

Frank, T. M. (1999). Comparative study of temporal resolution in the visual systems of mesopelagic crustaceans. *Biol. Bull.* **196**, 137-144. doi:10.2307/1542559

Frieder, C. A., Nam, S., Martz, T. R. and Levin, L. A. (2012). High temporal and spatial variability of dissolved oxygen and pH in a nearshore California kelp forest. *Biogeosciences* **9**, 3917-3930. doi:10.5194/bg-9-3917-2012

Gilly, W. F., Beman, J. M., Litvin, S. Y. and Robison, B. H. (2013). Oceanographic and biological effects of shoaling of the oxygen minimum zone. *Ann. Rev. Mar. Sci.* **5**, 393-420. doi:10.1146/annurev-marine-120710-100849

Grieshaber, M. K., Hardewig, I., Kreutzer, U. and Pörtner, H. O. (1994). Physiological and metabolic responses to hypoxia in invertebrates. *Rev. Physiol. Biochem. Pharmacol.* **125**, 43-147.

Hansen, B. W., Ea, S., Petersen, J. K. and Ellegaard, C. (2002). Invertebrate re-colonisation in Mariager Fjord (Denmark) after severe hypoxia. I. Zooplankton and settlement. *Ophelia* **56**, 197-213. doi:10.1080/00785236.2002.10409499

Hofmann, A. F., Peltzer, E. T., Walz, P. M. and Brewer, P. G. (2011). Hypoxia by degrees: establishing definitions for a changing ocean. *Deep Sea Res. Part 1* **58**, 1212-1226. doi:10.1016/j.dsr.2011.09.004

Hubbard, R., Brown, P. K. and Kropf, A. (1959). Action of light on visual pigments. *Nature* **183**, 442-446. doi:10.1038/183442a0

Lange, G. D. and Hartline, P. H. (1974). Retinal responses in squid and octopus. *J. Comp. Physiol. A* **93**, 19-36. doi:10.1007/BF00608757

Lecchini, D. (2011). Visual and chemical cues in habitat selection of sepioid larvae. *C. R. Biol.* **334**, 911-915. doi:10.1016/j.crvi.2011.08.003

Lecchini, D., Mills, S. C., Brié, C., Maurin, R. and Banaigs, B. (2010). Ecological determinants and sensory mechanisms in habitat selection of crustacean postlarvae. *Behav. Ecol.* **21**, 559-607. doi:10.1093/beheco/arq029

Levin, L. A. and Breitburg, D. L. (2015). Linking coasts and seas to address ocean deoxygenation. *Nat. Clim. Chang.* **5**, 401-403. doi:10.1038/nclimate2595

Levin, L. A., Liu, K. K., Emeis, K. C., Breitburg, D. L., Cloern, J., Deutsch, C., Giani, M., Goffart, A., Hofmann, E. E., Lachkar, Z. et al. (2015). Comparative biogeochemistry-ecosystem-human interactions on dynamic continental margins. *J. Mar. Syst.* **141**, 3-17. doi:10.1016/j.jmarsys.2014.04.016

Linsenmeier, R. A., Mines, A. H. and Steinberg, R. H. (1983). Effects of hypoxia and hypercapnia on the light peak and electroretinogram of the cat. *Invest. Ophthalmol. Vis. Sci.* **24**, 37-46.

McCormick, L. R. and Cohen, J. H. (2012). Pupil light reflex in the Atlantic brief squid, *Lolliguncula brevis*. *J. Exp. Biol.* **215**, 2677-2683. doi:10.1242/jeb.068510

McCormick, L. R. and Levin, L. A. (2017). Physiological and ecological implications of ocean deoxygenation for vision in marine organisms. *Philos. Trans. R. Soc. A* **375**, 20160322. doi:10.1098/rsta.2016.0322

McFarland, R. A. and Evans, J. N. (1939). Alterations in dark adaptation under reduced oxygen tensions. *Am. J. Physiol. Leg. Content* **127**, 37-50. doi:10.1152/ajplegacy.1939.127.1.37

McGowan, J. (1954). Observations on the sexual behavior and spawning of the squid, *Loligo opalescens*, at La Jolla, California. *Calif. Dep. Fish Game Fish. Bull.* **40**, 47-54.

Niven, J. E. and Laughlin, S. B. (2008). Energy limitation as a selective pressure on the evolution of sensory systems. *J. Exp. Biol.* **211**, 1792-1804. doi:10.1242/jeb.017574

Oesch, N. W. and Diamond, J. S. (2011). Ribbon synapses compute temporal contrast and encode luminance in retinal rod bipolar cells. *Nat. Neurosci.* **14**, 1555-1561. doi:10.1038/nn.2945

Pepe, I. M. (2001). Recent advances in our understanding of rhodopsin and phototransduction. *Prog. Retin. Eye Res.* **20**, 733-759. doi:10.1016/S1350-9462(01)00013-1

Rayer, B., Naynert, M. and Stieve, H. (1990). Phototransduction: different mechanisms in vertebrates and invertebrates. *J. Photochem. Photobiol. B* **7**, 107-148. doi:10.1016/1011-1344(90)85151-L

Robin, J.-P., Roberts, M., Zeidberg, L., Bloor, I., Rodriguez, A., Briceño, F., Downey, N., Mascaró, M., Navarro, M., Guerra, A. et al. (2014). Transitions during cephalopod life history: the role of habitat, environment, functional morphology, and behaviour. *Adv. Mar. Biol.* **67**, 361-437. doi:10.1016/B978-0-12-800287-2.00004-4

Schmidtko, S., Stramma, L. and Visbeck, M. (2017). Decline in global oceanic oxygen content during the past five decades. *Nature* **542**, 335-339. doi:10.1038/nature21399

Seibel, B. A. (2011). Critical oxygen levels and metabolic suppression in oceanic oxygen minimum zones. *J. Exp. Biol.* **214**, 326-336. doi:10.1242/jeb.049171

Seibel, B. A., Schneider, J. L., Kaartvedt, S., Wishner, K. F. and Daly, K. L. (2016). Hypoxia tolerance and metabolic suppression in oxygen minimum zone euphausiids: implications for ocean deoxygenation and biogeochemical cycles. *Integr. Comp. Biol.* **56**, 510-523. doi:10.1093/icb/icw091

Shapley, R. and Enroth-Cugell, C. (1984). Visual adaptation and retinal gain controls. *Prog. Retin. Res.* **3**, 263-346. doi:10.1016/0278-4327(84)90011-7

Steinberg, R. H. (1987). Monitoring communications between photoreceptors and pigment epithelial cells: effects of 'mild' systemic hypoxia (Friedenwald Lecture). *Investig. Ophthalmol. Vis. Sci.* **12**, 1888-1904.

Sulkin, S. (1984). Behavioral basis of depth regulation in the larvae of brachyuran crabs. *Mar. Ecol. Prog. Ser.* **15**, 181-205. doi:10.3354/meps015181

Tyler, R. M., Brady, D. C. and Targett, T. E. (2009). Temporal and spatial dynamics of diel-cycling hypoxia in estuarine tributaries. *Estuaries Coasts* **32**, 123-145. doi:10.1007/s12237-008-9108-x

Warrant, E. J. and Johnsen, S. (2013). Vision and the light environment. *Curr. Biol.* **23**, R990-R994. doi:10.1016/j.cub.2013.10.019

Wishner, K. F., Outram, D. M., Seibel, B. A., Daly, K. L. and Williams, R. L. (2013). Zooplankton in the eastern tropical north Pacific: boundary effects of oxygen minimum zone expansion. *Deep Sea Res. Part I Oceanogr. Res. Pap.* **79**, 122-140. doi:10.1016/j.dsr.2013.05.012

Wishner, K. F., Seibel, B. A., Roman, C., Deutsch, C., Outram, D., Shaw, C. T., Birk, M. A., Mislan, K. A. S., Adams, T. J., Moore, D. et al. (2018). Ocean deoxygenation and zooplankton: very small oxygen differences matter. *Sci. Adv.* **4**, eaau5180. doi:10.1126/sciadv.aau5180

Wong-Riley, M. (2010). Energy metabolism of the visual system. *Eye Brain* **2**, 99-116. doi:10.2147/EB.S9078

Wu, R. S. S. (2002). Hypoxia: from molecular responses to ecosystem responses. *Mar. Pollut. Bull.* **45**, 35-45. doi:10.1016/S0025-326X(02)00061-9

Yannicelli, B., Paschke, K., González, R. R. and Castro, L. R. (2013). Metabolic responses of the squat lobster (*Pleuroncodes monodon*) larvae to low oxygen concentration. *Mar. Biol.* **160**, 961-976. doi:10.1007/s00227-012-2147-7

Zeidberg, L. D. and Hamner, W. M. (2002). Distribution of squid paralarvae, *Loligo opalescens* (Cephalopoda: Myopsida), in the Southern California Bight in the three years following the 1997-1998 El Niño. *Mar. Biol.* **141**, 111-112. doi:10.1007/s00227-002-0813-x

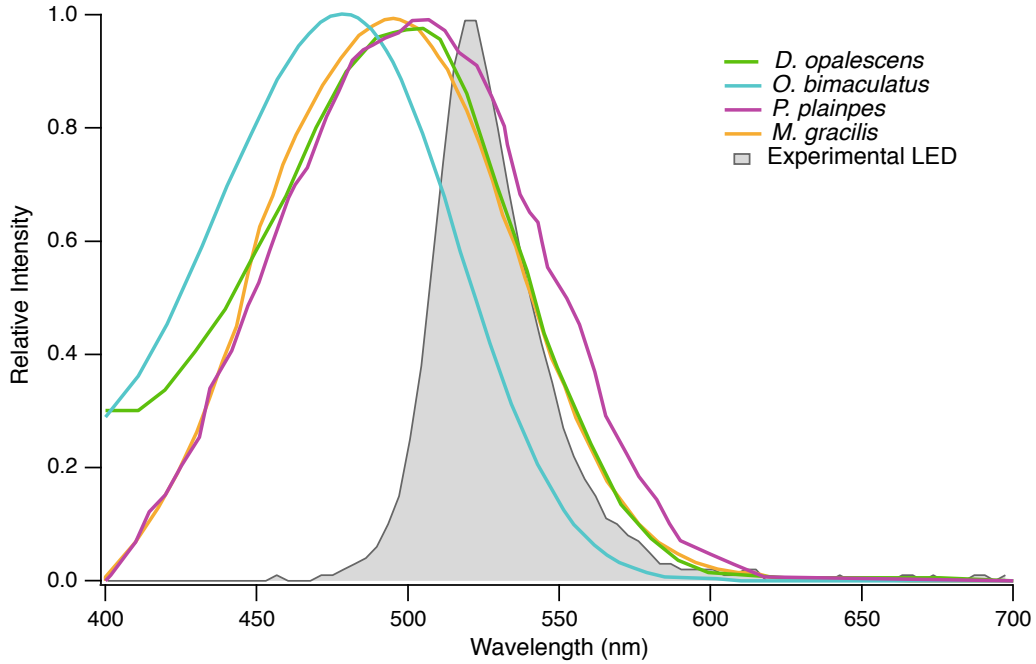

Fig S1. Comparison of experimental light and spectral sensitivities of each species.
Estimated spectral sensitivities of the market squid, *Doryteuthis opalescens* (green line); the octopus, *Octopus bimaculatus* (teal line); the tuna crab, *Pleuroncodes planipes* (magenta line); and the graceful rock crab, *M. gracilis* (orange line), in comparison to the spectrum of the green LED (gray line and shading) used in all experiments (525 nm, 35 nm FWHM; Thorlabs). Data for spectral sensitivities were obtained or modified from existing literature for the same species, or a taxonomically related species with similar life history and habitat depth: *D. opalescens* from sensitivity of *Doryteuthis pealeii* (Hubbard et al., 1959); *O. bimaculatus* from sensitivity of *O. vulgaris* (Brown and Brown, 1958); *P. planipes* (Fernandez, 1973); and *M. gracilis* from *Cancer irroratus* (Cronin and Forward, 1988). These spectra were used to determine the species-specific photon flux density.

Table S1. Statistical results of response-irradiance relationships.

Statistical comparisons of light series tests (Figs. 4, 5) conducted on the larvae of the market squid, *D. opalescens* (green); the octopus, *O. bimaculatus* (teal); the tuna crab, *P. planipes* (magenta); and the graceful rock crab, *M. gracilis* (orange). Differences between visual responses at three oxygen conditions (normoxia, ~22 kPa/~265 μmol kg^{-1}; intermediate reduction of pO_2, ~6.5 kPa/~95 μmol kg^{-1}; and low pO_2, ~3.5 kPa/~55 μmol kg^{-1}) at each experimental irradiance [in species-specific photon flux density (μmol photons m^{-2} s^{-1})] were determined using Kruskal-Wallis tests in each species. Results are presented for the light series visual responses normalized to both the maximum value of normoxia ("Normalized to normoxia"; Fig. 4) and the maximum value within each oxygen condition ("Normalized within each condition"; Fig 5). Significant values ($p < 0.05$) are presented in bold. Abbreviations: df = degrees of freedom; NA = not applicable; PFD = photon flux density.

df = 2		Squid PFD	0.033	0.296	0.557	0.815	1.073	1.327	1.581	1.834	2.087
D. opalescens	Normalized to normoxia	Chi squared	2.808	8.000	8.769	8.000	8.000	8.346	8.346	8.346	8.649
		p-value	0.246	**0.018**	**0.012**	**0.018**	**0.018**	**0.015**	**0.015**	**0.015**	**0.013**
	Normalized within each condition	Chi squared	1.423	4.154	3.846	1.654	4.962	2.808	0.269	3.039	NA
		p-value	0.491	0.125	0.146	0.437	0.084	0.246	0.874	0.219	NA
df = 2		Octopus PFD	0.024	0.209	0.393	0.576	0.758	0.938	1.117	1.296	1.474
O. bimaculatus	Normalized to normoxia	Chi squared	2.400	6.489	7.200	6.489	6.489	6.489	6.489	6.489	6.713
		p-value	0.301	**0.039**	**0.027**	**0.039**	**0.039**	**0.039**	**0.039**	**0.039**	**0.035**
	Normalized within each condition	Chi squared	5.067	2.222	5.067	5.600	4.267	2.756	5.689	1.689	NA
		p-value	0.079	0.329	0.079	0.061	0.118	0.252	0.058	0.430	NA
df = 2		Tuna Crab PFD	0.036	0.323	0.608	0.891	1.173	1.450	1.727	2.004	2.280
P. planipes	Normalized to normoxia	Chi squared	4.500	6.731	5.654	6.269	6.000	6.731	6.000	7.731	8.290
		p-value	0.105	**0.035**	0.059	**0.044**	**0.050**	**0.035**	**0.050**	**0.021**	**0.016**
	Normalized within each condition	Chi squared	1.500	0.269	1.192	3.136	0.615	0.115	0.154	1.631	NA
		p-value	0.472	0.874	0.551	0.209	0.735	0.944	0.926	0.443	NA
df = 2		Crab PFD	0.032	0.288	0.542	0.794	1.045	1.292	1.539	1.786	2.031
M. gracilis	Normalized to normoxia	Chi squared	12.737	15.431	14.794	14.500	14.500	14.222	14.222	14.500	14.005
		p-value	**0.002**	**0.000**	**0.001**	**0.001**	**0.001**	**0.001**	**0.001**	**0.001**	**0.001**
	Normalized within each condition	Chi squared	4.774	1.433	2.151	0.693	2.821	0.693	3.468	2.331	NA
		p-value	0.092	0.488	0.341	0.707	0.244	0.707	0.177	0.312	NA